Proceedings of the 2nd International Conference on Fluid Flow and Thermal Science (ICFFTS'21)
~~Seoul, South Korea~~ Virtual Conference - November 24- 26, 2021
Paper No. 114
DOI: 10.11159/icffts21.114

Analysis of Vorticity Distribution in a Closed Partially Porous Domain

Abhijit Verma
Indian Institute of Science Bangalore
C. V. Raman Road, Bengaluru-560012, India
abhijitverma@iisc.ac.in

Abstract **-** We analyse the steady state vorticity distribution in a closed partially porous square domain upon creating a vortex sheet on the top boundary. Following one domain approach, the transport of vorticity in the coupled clear and porous media is governed by generalized porous flow model. Effect of Reynold number $Re = \{10^2, 10^3\}$, Darcy number $Da = \{10^{-2}, 10^{-4}\}$, and dimensionless thickness of porous layer H = {.01, .25, .50, .75} on the vorticity field are analysed. It is observed that a uniform vorticity region develops in the core of the domain at high Reynold and Darcy numbers $Re = 10^3$, $Da = 10^{-2}$. With decrease in Darcy number to 10^{-4}, region of uniform vorticity forms above the porous layer. As the thickness of porous layer increases, this region shifts towards the top-right corner. Also, vorticity with opposite sign are observed near the top boundary and interface between free fluid and porous medium. Furthermore, minimum vorticity along the top boundary decreases with *Da*, increases with *Re*, and decreases as H increases.

Keywords**:** Vortex sheet, Vorticity distribution, Partially porous closed domain, Generalized porous flow model

1. Introduction

In closed domain, recirculating flows generated by imposing vortex sheet (in other words, uniform translation) on a section of the boundary are almost canonical flow problems and have been analysed extensively. For instance, Gatski et al. [1] presented evolution of vorticity and velocity field with time for Reynold number 400 in square as well as rectangular domain (aspect ratio 0.5) whose top boundary is suddenly applied with a sheet of infinite vorticity. They also pointed out that time required to reach steady state is proportional to Reynold number. Ghia et al. [2] showed vorticity distribution in a square domain for Reynold number in the range 10^2 to 10^4. Botella et al. [3] presented highly accurate benchmark solution for vorticity, pressure and velocity field in a square domain for Reynold number 10^3. Sahin et al. [4] showed the vorticity distribution in a square domain for Reynold number 0 to 10^4. They also showed the evolution of flow structure with time. Erturk et al. [5] demonstrated the effect of Reynold number 10^3 to 21×10^3 on vorticity at the centre of primary vortex. Cheng et al. [6] investigated vortex structure and vorticity distribution in rectangular domain for Reynold number 10^{-2} to 5×10^3 and aspect ratio 0.1 to 7. Patil et al. [7] analysed stream function and vorticity contours in a deep domain for Reynold number 50 to 3200 and aspect ratio 1.5 to 4. Nevertheless, in several technological applications, the domain may be partially occupied with porous medium. To the best of author's knowledge, no study has been carried out on internal recirculation with vorticity distribution in partially porous domain with closed boundary.

In this paper, we analyse the vorticity field in a closed square domain with porous layer placed on the bottom boundary. Vortices in the domain is maintained by applying uniform translation condition on the top boundary. Reynold number, Darcy number, and dimensionless thickness of porous layer are the key parameters in this analysis. Taking one-domain approach, vorticity transport in the coupled clear and porous media is modelled by velocity-vorticity formulation based on the generalized porous flow equation.

2. Mathematical Model

As shown in Figure 1, we analyse vorticity field ω (x, y) in a unit square domain with porous medium present in (0, 1) × (0, H). The recirculation in the domain is sustained by the uniform and constant tangential velocity applied on the top section of the boundary. Following one-domain approach, fluid motion in the entire domain is described in terms of dimensionless velocity $\mathbf{v} = (u, v)$ and vorticity ω by generalized momentum equation [8, 9] in the form

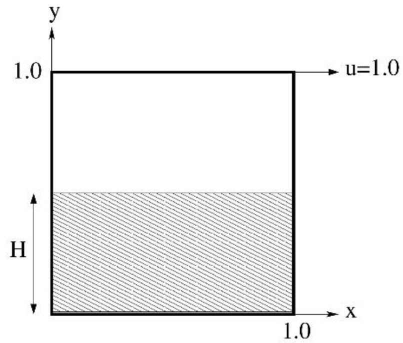

Fig. 1: Schematic of closed partially porous square domain with uniform translation of top boundary.

$$\frac{\partial u}{\partial \mathrm{x}}+\frac{\partial v}{\partial \mathrm{y}}= 0 \tag{1}$$

$$\frac{\partial v}{\partial \mathrm{x}}-\frac{\partial u}{\partial \mathrm{y}}= \omega \tag{2}$$

$$\begin{aligned}\frac{\partial \omega}{\partial t}+u\frac{\partial}{\partial \mathrm{x}}\left(\frac{\omega}{\varphi^*}\right)+v\frac{\partial}{\partial \mathrm{y}}\left(\frac{\omega}{\varphi^*}\right)=\frac{\varphi^*}{Re}\left(\frac{\partial^2}{\partial \mathrm{x}^2}\left(\frac{\omega}{\varphi^*}\right)+\frac{\partial^2}{\partial y^2}\left(\frac{\omega}{\varphi^*}\right)\right)-\left(\frac{\varphi^*}{ReDa^*}+\frac{0.143|\mathbf{v}|}{\sqrt{\varphi^* Da^*}}\right)\omega \\ +\frac{2\varphi^*}{Re}\left(\frac{\partial^2}{\partial \mathrm{x}^2}\left(\frac{1}{\varphi^*}\right)\frac{\partial u}{\partial \mathrm{y}}-\frac{\partial^2}{\partial y^2}\left(\frac{1}{\varphi^*}\right)\frac{\partial v}{\partial \mathrm{x}}+\frac{\partial^2}{\partial \mathrm{x}\,\partial y}\left(\frac{1}{\varphi^*}\right)\left(\frac{\partial v}{\partial \mathrm{y}}-\frac{\partial u}{\partial \mathrm{x}}\right)\right) \\ -\frac{0.143}{\sqrt{\varphi^* Da^*}}\left(v\frac{\partial|\mathbf{v}|}{\partial \mathrm{x}}-u\frac{\partial|\mathbf{v}|}{\partial \mathrm{y}}\right)\end{aligned} \tag{3}$$

where Re, φ^*, and Da^* are Reynold number, porosity field and Darcy number field.

It is evident that the system of equations (1) - (3) reduces to velocity and vorticity formulation by Navier-Stokes equation for $\varphi^* \rightarrow 1$ and $Da^* \rightarrow \infty$. Here, the sharp interface at y = H is replaced with a thin transition layer across which the porosity and Darcy number vary continuously. For a given porosity φ and Darcy number Da of the porous medium, in the domain, porosity and Darcy number fields are modelled as

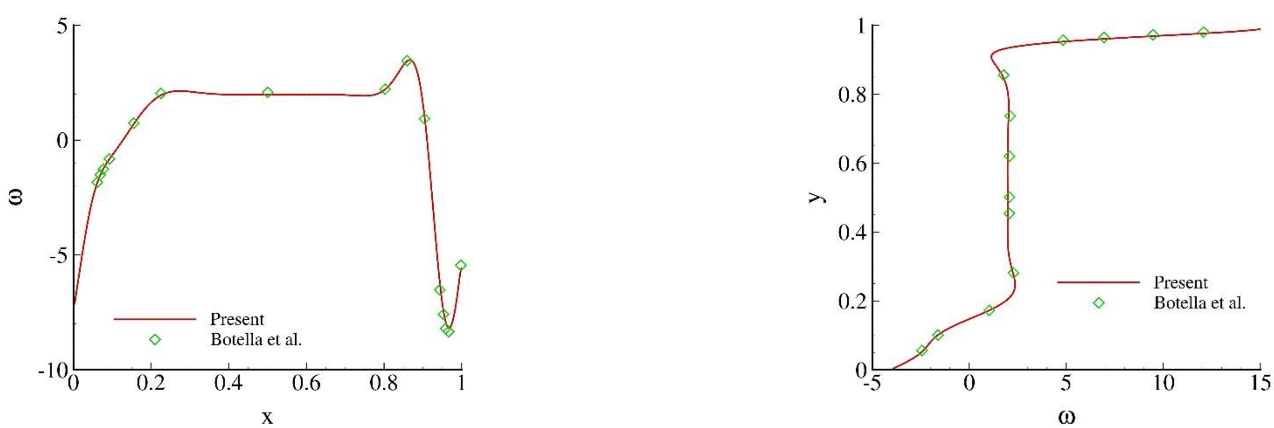

Fig. 2: Comparison of vorticity profile along the midlines y = 0.5 and x = 0.5 with those of Botella et al. [3] for $Re = 10^3$, and H = .001.

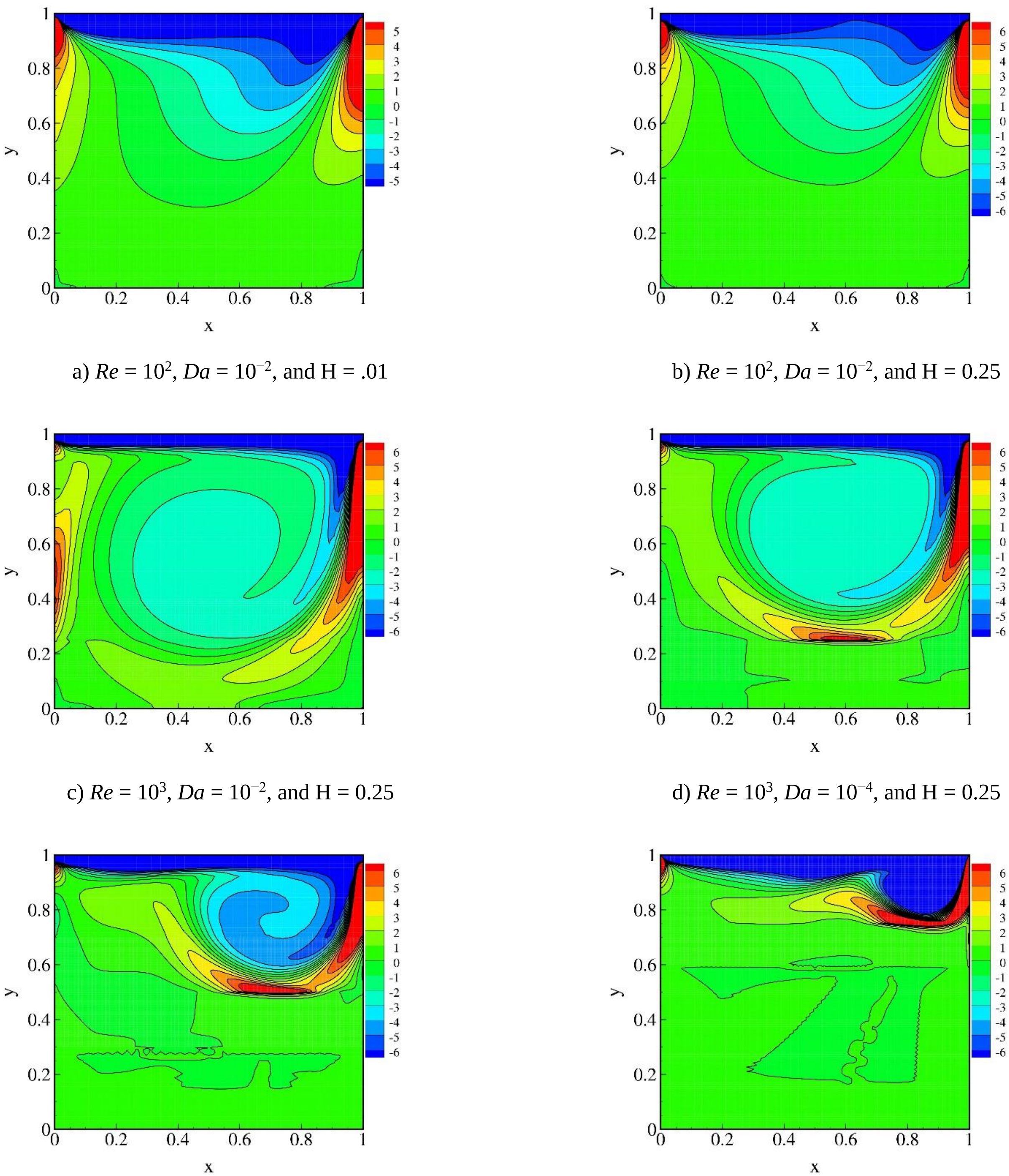

a) $Re = 10^2$, $Da = 10^{-2}$, and H = .01

b) $Re = 10^2$, $Da = 10^{-2}$, and H = 0.25

c) $Re = 10^3$, $Da = 10^{-2}$, and H = 0.25

d) $Re = 10^3$, $Da = 10^{-4}$, and H = 0.25

e) $Re = 10^3$, $Da = 10^{-4}$, and H = 0.50

f) $Re = 10^3$, $Da = 10^{-4}$ and H = 0.75

Fig. 3: Change in vorticity contours with *Re*, *Da*, and H.

$$\varphi^*(\mathrm{x,y}) = \frac{1 + \varphi \mathrm{e}^{-\theta(y-H)}}{1 + \mathrm{e}^{-\theta(y-H)}} \tag{4}$$

$$Da^*(\mathrm{x,y}) = \frac{\varphi^{*3}(1-\varphi)^2 Da}{\varphi^3(1-\varphi^*)^2} \tag{5}$$

where θ is an arbitrary parameter. As φ^* and Da^* undergo rapid changes in the transition region, the governing equations are discretized on quadtree grid to facilitate the extra resolution near the interface efficiently. To obtain the steady state vorticity field, taking stationary flow field as initial condition, we iterate in time until the first norm of the difference in vorticity field at two successive time level goes below 10^{-7}. In order to verify the computer code, in Figure 2, we compare the vorticity profile along the straight lines passing through the geometric centre of the domain for $Re = 10^3$ and H = .001 against the benchmark solutions available in the literature. The present results are found to be in very good agreement with the numerical solutions of Botella et al. [3].

3. Results and Discussion

We present simulation results for $Re = \{10^2, 10^3\}$, $Da = \{10^{-2}, 10^{-4}\}$, and dimensionless thickness of porous layer H = {.01, .25, .50, .75}. The porosity is held constant at $\varphi = 0.7$. The domain (Figure 1) is discretized using hybrid grid with extra resolution near the interface y = H. The demand for finer grid near the interface increases as Darcy number decreases. To perform all these simulations, grid size and time step are varied in the range $[2^{-6}, 2^{-9}]$ and $[10^{-3}, 10^{-5}]$ respectively. The value of θ, associated with equation (4), is taken as 300.

In Figures 3a - 3f, we show vorticity field in the steady state for different *Re*, *Da* and H. We also plot the corresponding vorticity distribution along the top boundary in Figure 4. For low Reynold number $(Re = 10^2)$, introduction of porous medium with high permeability $(Da = 10^{-2})$ and small thickness $(\mathrm{H} = 0.25)$ in the lower region increases the vorticity in the upper section of the domain slightly. However, this effect doesn't propagate upto the top side and vorticity remains almost unchanged along the top boundary. Increase in Reynold number $(Re = 10^3 \leftarrow 10^2)$ changes the vorticity distribution in the domain significantly. A uniform vorticity region in the central part of the domain and multiple regions of high vorticity gradients near the boundary are developed (Figure 3c). Vorticity distribution along the top boundary also changes substantially. As the resistance of the porous medium increases i.e. Darcy number decreases $(Da = 10^{-4} \leftarrow 10^{-2})$, vorticity in the porous layer approaches to zero and region of high vorticity gradient appears near the interface as well (Figure 3d). Magnitude of vorticity reduces slightly in the second half of top boundary $(\mathrm{x} > 0.5)$. With increase in thickness of porous layer $(\mathrm{H} = 0.5 \leftarrow 0.25)$, boundary layer associated with the interface shifts accordingly. Also, the region of uniform vorticity shrinks in size and moves towards the right corner (Figure 3e). The trend continues with further increase in thickness

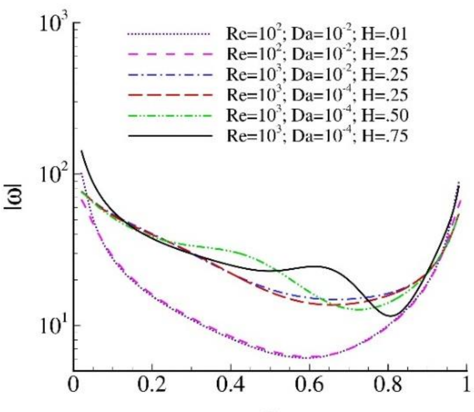

Fig. 4: Change in vorticity along the top boundary with *Re*, *Da* and H.

of porous layer ($H = 0.75 \leftarrow 0.5$) as evident by the high density of the vorticity contours between the interface and region of uniform vorticity in Figure 3f. For $Da = 10^{-4}$ and H = {0.5, 0.75}, as shown in Figure 4, profile of |ω| along the top boundary shows local maxima and minima in the right half section of the boundary. The minima decreases and its location shifts towards the right corner with increase in H.

4. Conclusion

We have analysed the steady-state distribution of vorticity for different Reynold number, Darcy number, and thickness of porous layer in a closed square domain partially filled with porous medium. Upon placing a sheet of infinite vorticity on the top boundary, the vorticity diffuses and advects in the domain. Adopting one-domain approach, the transport of vorticity in the entire domain is modelled by velocity-vorticity formulation of generalized porous flow model. It is observed that increase in *Re* from 10^2 to 10^3 leads to formation of uniform vorticity region in the centre of the domain. With reduction in *Da* from 10^{-2} to 10^{-4}, vorticity in the porous layer becomes negligible and steep change in vorticity occurs near the interface. For $Da = 10^{-4}$, this region moves towards the top-right corner with increase in thickness of porous layer. The size of this region also decreases as thickness increases. Additionally, magnitude of vorticity (|ω|) along the top boundary increases significantly as *Re* changes from 10^2 to 10^3. With drop in *Da* to 10^{-4}, |ω| decreases slightly in the downstream part of top boundary. For $Da = 10^{-4}$, as thickness increases beyond 0.25, |ω| ceases to show parabolic kind of distribution along the top boundary. Moreover, the location of minimum |ω| continues to shift towards the right corner with increase in thickness of porous layer.

References

[1] Thomas B Gatski, Chester E Grosch, and Milton E Rose. A numerical study of the two-dimensional Navier-Stokes equations in vorticity-velocity variables. *Journal of Computational Physics*, 48(1):1–22, 1982.

[2] UKNG Ghia, Kirti N Ghia, and CT Shin. High-re solutions for incompressible flow using the Navier-Stokes equations and a multigrid method. *Journal of computational physics*, 48(3):387–411, 1982.

[3] O Botella and R Peyret. Benchmark spectral results on the lid-driven cavity flow. *Computers & Fluids*, 27(4):421–433, 1998.

[4] Mehmet Sahin and Robert G Owens. A novel fully implicit finite volume method applied to the lid-driven cavity problem—part i: High Reynolds number flow calculations. *International journal for numerical methods in fluids*, 42(1):57–77, 2003.

[5] Ercan Erturk, Thomas C Corke, and Cihan Gökçöl. Numerical solutions of 2-d steady incompressible driven cavity flow at high Reynolds numbers. *International journal for Numerical Methods in fluids*, 48(7):747–774, 2005.

[6] M Cheng and KC Hung. Vortex structure of steady flow in a rectangular cavity. *Computers & fluids*, 35(10):1046–1062, 2006.

[7] DV Patil, KN Lakshmisha, and B Rogg. Lattice boltzmann simulation of lid-driven flow in deep cavities. *Computers & fluids*, 35(10):1116–1125, 2006.

[8] Zhaoli Guo and TS Zhao. Lattice boltzmann model for incompressible flows through porous media. *Physical review E*, 66(3):036304, 2002.

[9] Antony A Hill and Magda Carr. Nonlinear stability of the one-domain approach to modelling convection in superposed fluid and porous layers. *Proceedings of the Royal Society A: Mathematical, Physical and Engineering Sciences*, 466(2121):2695–2705, 2010.